



Published in final edited form as:

Hypertension. 2017 November ; 70(5): 990–997. doi:10.1161/HYPERTENSIONAHA.117.09923.

Selective Deletion of Renin-b in the Brain Alters Drinking and Metabolism

Keisuke Shinohara¹, Pablo Nakagawa^{1,*}, Javier Gomez^{1,*}, Donald A. Morgan¹, Nicole K. Littlejohn¹, Matthew D. Folchert¹, Benjamin J. Weidemann¹, Xuebo Liu¹, Susan A. Walsh², Laura L. Ponto², Kamal Rahmouni^{1,3}, Justin L. Grobe^{1,3}, and Curt D. Sigmund^{1,3}

¹Department of Pharmacology, Roy J. and Lucille. Carver College of Medicine, University of Iowa, Iowa City

²Department of Radiology, Roy J. and Lucille. Carver College of Medicine, University of Iowa, Iowa City

³UIHC Center for Hypertension Research, Roy J. and Lucille. Carver College of Medicine, University of Iowa, Iowa City

Abstract

The brain specific isoform of renin (Ren-b), has been proposed as a negative regulator of the brain renin-angiotensin system (RAS). We analyzed mice with a selective deletion of Ren-b which preserved expression of the classical renin (Ren-a) isoform. We reported that Ren-b^{Null} mice exhibited central RAS activation and hypertension through increased expression of Ren-a, but the dipsogenic and metabolic effects in Ren-b^{Null} mice are unknown. Fluid intake was similar in control and Ren-b^{Null} mice at baseline and both exhibited an equivalent dipsogenic response to DOCA-salt. Dehydration promoted increased water intake in Ren-b^{Null} mice, particularly after DOCA-salt. Ren-b^{Null} and control mice exhibited similar body weight when fed a chow diet. However, when fed a high fat diet, male Ren-b^{Null} mice gained significantly less weight than control mice, an effect blunted in females. This difference was not due to changes in food intake, energy absorption or physical activity. Ren-b^{Null} mice exhibited increased resting metabolic rate concomitant with increased uncoupled protein 1 expression and sympathetic nerve activity to the interscapular brown adipose tissue (BAT), suggesting increased thermogenesis. Ren-b^{Null} mice were modestly intolerant to glucose and had normal insulin sensitivity. Another mouse model with markedly enhanced brain RAS activity (sRA mice) exhibited pronounced insulin sensitivity concomitant with increased BAT glucose uptake. Altogether, these data support the hypothesis that the brain RAS regulates energy homeostasis by controlling resting metabolic rate, and that Ren-b deficiency increases brain RAS activity. Thus, the relative level of expression of Ren-b and Ren-a may control activity of the brain RAS.

Corresponding Author: Curt D. Sigmund, Ph.D., Department of Pharmacology, Roy J. and Lucille A. Carver College of Medicine, University of Iowa, 51 Newton Rd., 2-340 BSB, Iowa City, Iowa, 52242, Phone: 319-335-7946, Fax: 319-335-8930, curt-sigmund@uiowa.edu.

*Denotes Equal Contribution

Conflict of Interest/Disclosure: None

Keywords

Renin; angiotensin II; brain; sympathetic nervous system; hypertension

Introduction

It is well recognized that the renin-angiotensin system (RAS) in the brain controls cardiovascular function by regulating fluid homeostasis and the sympathetic nervous system (SNS). Intracerebroventricular administration of angiotensin-II (Ang-II) causes a potent dipsogenic response through its action in forebrain nuclei such as the subfornical organ and is mediated by AT1 receptors.¹⁻³ Similarly, AT1 receptor activation causes increased sympathetic activity to the vasculature, heart and kidney.⁴ Activation of the brain RAS has been recently shown to have metabolic effects, and the mechanisms controlling the dipsogenic vs metabolic responses to brain RAS activation are mediated by divergent efferent pathways.⁵ Interestingly, brain RAS-elicited metabolic responses are mediated by a complex interplay between central AT1 receptors and adipose tissue AT2 receptors, suggesting a brain/adipose axis regulated by the brain RAS.⁶ Previous studies suggested a physiological link between Ang-II and leptin signaling in the regulation of the SNS⁷, and AT1 receptor signaling in leptin receptor containing cells of the arcuate nucleus regulates resting metabolic rate.⁸

Direct blockade of brain RAS activity by intracerebroventricular administration of renin inhibitors, angiotensin converting enzyme (ACE) inhibitors, or AT1 receptor blockers lowers blood pressure in many models of hypertension.^{9,10} This has been interpreted as evidence for an involvement of the brain RAS in hypertension. These data combined with the absence of significant blood pressure effects when the same blockers are injected into the brain of normal animals has been interpreted to mean that brain RAS activity is increased in hypertension. By analogy, baseline activity of the brain RAS is low under normal conditions, implying there must be some mechanism for the tight regulation of brain RAS activity and for RAS activation in response to physiological or pathological cues. We recently described a potentially novel mechanism regulating brain RAS activity.¹¹ This mechanism involves controlling which promoter and transcriptional start site is used to transcribe the renin gene in the brain. Under baseline conditions, transcription of renin mRNA in the brain occurs at an alternative promoter compared with the promoter used to transcribe renin in renal juxtaglomerular cells.^{12,13} The product of this transcript (termed Ren-b) is brain-specific, lacks the signal peptide and is therefore unlikely to be secreted. The predicted translation product of Ren-b lacks the first third of the prosegment and was shown to be enzymatically active.¹² However, it was unclear if Ren-b expression is physiologically significant.

In order to define a function for Ren-b, we deleted the DNA surrounding and including the Ren-b promoter.¹¹ Surprisingly, removing the capacity for Ren-b expression resulted in increased expression of Ren-a, encoding preprorenin. This activation of Ren-a occurs concomitantly with increased brain RAS activity and hypertension, suggesting an inhibitory model of renin gene regulation which suppresses RAS activity in the brain. Supporting this model, there is a switch in expression from primarily Ren-b in the brain of untreated

wildtype mice to the expression of primarily Ren-a within the brain in response to DOCA-salt treatment.¹⁴ This suggests a novel mechanism by which certain physiological cues causes a disinhibition of Ren-a.

It is notable that DOCA-salt hypertension is characterized by increased brain RAS activity because the hypertension can be blocked by brain-specific administration of ACE inhibitors or AT1 receptor blockers.^{15,16} Similarly, the hypertension in Ren-b^{Null} mice can be blocked by renin inhibitors, ACE inhibitors or AT1 receptor blockers suggesting some similarity between the models.¹¹ DOCA-salt also increases resting metabolic rate (RMR) that is blunted by ICV infusion of losartan.¹⁷ Moreover, like the DOCA-salt model, double transgenic sRA mice, which over-express a) human angiotensinogen at its normal sites of synthesis, and b) renin-a selectively in the brain, exhibit severe hypertension, increased fluid intake, and increased RMR.^{5,18} It is notable that the increased Ang-II in sRA mice is brain-specific and is due to over-expression of Ren-a, but not Ren-b. Indeed, there was no manipulation of endogenous Ren-b in sRA mice. In this study we hypothesize that mice carrying a deficiency in Ren-b (Ren-b^{Null}) mice develop several cardinal phenotypes evoked by increased activity of the brain RAS. We tested the specific hypothesis that Ren-b^{Null} mice exhibit increased fluid intake and resting metabolic rate.

Methods

Details of the drinking studies, analysis of blood chemistry and urinary steroids, measures and calculations to determine metabolic rate, measures of brown adipose tissue sympathetic nerve activity, studies to assess glucose tolerance, insulin sensitivity and glucose uptake, and methods for Western blot and RNA isolation are provided in the Online Only Data Supplement.

Renin-b^{Null} mice

Generation, validation and initial characterization of Ren-b^{Null} mice was previously reported.¹¹ Mice carrying the Ren-b^{Null} allele were maintained by backcross breeding to C57BL/6J, and heterozygotes were intercrossed to generate the Ren-b^{Null} mice. Male and female mice were fed standard laboratory chow (NIH-31 modified 6 kcal% mouse diet, Harlan Teklad) and tap water *ad libitum*. For high fat diet studies, mice were fed D12451 (45 kcal% fat, Research Diets) for 16 weeks beginning at 6 weeks of age. All studies were approved by the University of Iowa Animal Care and Use Committee and were performed in accordance with the National Institutes of Health Guide for the Care and Use of Laboratory Animals.

Statistics

Data were analyzed using t-tests or 1-way or 2-way ANOVA with repeated measures as appropriate, followed by Tukey multiple-comparisons procedures. ANOVA results are presented in each figure legend. ANCOVA was used to analyze resting metabolic rate data using SPSS. All data are presented as mean \pm SEM. Differences were considered significant if $p < 0.05$. Where appropriate individual data points are plotted in dot/whisker plots and individual statistical tests are noted in the figure legend.

Results

We first measured fluid intake in a cohort of Ren-b^{Null} and control mice using a two bottle choice paradigm where mice were given a choice of either tap water or 0.15M saline. There was no significant change in baseline fluid intake or saline preference in Ren-b^{Null} mice (Table S1). Similarly, there were no changes in urine volume, urinary sodium excretion or potassium excretion in Ren-b^{Null} mice, nor changes in urinary corticosterone or aldosterone. Because the level of brain RAS activity in Ren-b^{Null} mice is likely to be lower than in sRA mice, which exhibit brain-selective Ang-II overexpression, we asked if a further stimulus was required to unmask an augmented response in Ren-b^{Null} mice. DOCA-salt, which activates the brain RAS¹⁷, caused an increase in the fluid intake in both groups of mice, but did not cause an exaggerated increase in fluid intake in Ren-b^{Null} mice (Table S1). As expected, urine volume and urinary sodium excretion increased in both Ren-b^{Null} and control mice after DOCA-salt. Next, we tested the drinking responses to a dehydration stimulus by measuring water intake after mice were deprived of fluids for 18 hours. Water consumption increased at a similar rate at first but began to diverge by 30 minutes (Figure 1A). After 2 hours, there was a trend for increased water consumption after dehydration in Ren-b^{Null} mice but this difference did not reach significance (Figure 1B). On the contrary, DOCA-salt treated Ren-b^{Null} mice subjected to dehydration exhibited augmented water intake compared with DOCA-salt treated control mice also subjected to dehydration. These data suggest that activation of brain RAS activity caused by Ren-b deficiency may be insufficient on its own to stimulate water intake whereas dehydration provides a stimulus or behavioral sensitization which augments the dipsogenic response in the model.

To assess if there are alterations in metabolic responses in Ren-b^{Null} mice, we recorded body weight from 6 to 22 weeks of age. There was no difference in body weight or fat mass in either male (Figure 2A–C) or female (Figure 2D–F) Ren-b^{Null} mice fed chow diet. However, male Ren-b^{Null} mice gained significantly less weight and exhibited decreased fat mass in response to 45% high fat diet (HFD). Both Ren-b^{Null} and control mice exhibited increased interscapular brown adipose tissue (BAT), perigenital white adipose tissue (WAT) and inguinal WAT mass in response to HFD (Table S2). In males, there was a blunting of the increased inguinal WAT mass depot in Ren-b^{Null} mice. Interestingly, HFD caused a marked increase in the size of the liver in control mice that was blunted in male Ren-b^{Null} (Table S2). The change in liver size only occurred in males.

Body weight in female Ren-b^{Null} and control mice fed HFD appeared to increase at a similar rate until about 18 weeks of age when they started to diverge (Figure 2D). The rate of weight gain in response to HFD was less in female mice than in male mice. At 22 weeks of age, HFD caused an increase in body weight and fat mass in control mice that was blunted in female Ren-b^{Null} mice (Figure 2E–F). Like males, female Ren-b^{Null} and control mice exhibited increased interscapular brown adipose tissue (BAT), perigenital white adipose tissue (WAT) and inguinal WAT mass in response to HFD (Table S2). However, unlike males, there was a blunted increase in perigenital WAT in female Ren-b^{Null} mice.

The difference in body weight was not due to differences in food consumption (Figure 3A), energy absorption (Figure 3B), or physical activity (Figure 3C) between male Ren-b^{Null} and

control mice. We next measured resting metabolic rate (RMR) by respirometry plotting kcal/hr of O₂ vs body weight in a cohort of 46 Ren-b^{Null} and 53 control male and female mice fed either chow or HFD (Figure 3D). Regression analysis revealed an increase in RMR in Ren-b^{Null} mice that was confirmed when ANCOVA-adjusted RMR was considered (Figure 3E). Given the increase in RMR, we asked if there was increased expression of uncoupling protein 1 (UCP1) mRNA and protein in BAT in Ren-b^{Null} mice. UCP1 mRNA (Figure 4A) and protein (Figure 4B) were significantly increased in BAT from Ren-b^{Null} mice fed either chow or HFD. There was no increase in UCP1 in perigenital WAT (data not shown). Consistent with the increase in RMR and UCP1 in BAT, sympathetic nerve activity to the BAT was elevated in Ren-b^{Null} mice fed chow (Figure 4C–D).

Because RAS modulators have consistently beneficial effects on glycemic control in humans¹⁹, we examined if under chow conditions, there were changes in glucose tolerance and insulin sensitivity in Ren-b^{Null} mice. When injected at 1g/kg, there was no evidence for glucose intolerance in Ren-b^{Null} mice (Figure 5A). However, this was modestly worsened when glucose was injected at 2g/kg (Figure 5B), such that the area under the curve was significantly increased (Figure 5C). There was a modest increase in insulin sensitivity when insulin was injected at 1U/kg, but not at 0.5U/kg (Figure 5D,E), but the decrease in the area under the curve did not reach significance (Figure 5F, P=0.08). No differences in plasma insulin levels were observed in fasting or Ad-libitum fed Ren-b^{Null} mice (data not shown).

Given the trend for increased insulin sensitivity, we repeated the glucose and insulin tolerance tests in sRA mice which exhibit a much greater increase in brain RAS activity. Although there was only a modest improvement in glucose tolerance (Figure 6A), sRA mice exhibited profound sensitivity to insulin (Figure 6B). Note that only a low dose of insulin was tested because several sRA mice became distressed and the experiment had to be terminated before completion. Differences in area under the curve comparing sRA and control mice was significant (P=0.017). Consistent with increased insulin sensitivity, sRA mice exhibited an increase in glucose uptake in BAT (Figure 6C).

Discussion

There are several main findings of the current study. First, whereas Ren-b^{Null} mice do not exhibit changes in fluid intake or salt preference under baseline conditions or after DOCA-salt, 18 hours of dehydration caused increased water intake in Ren-b^{Null} mice. Second, Ren-b^{Null} mice exhibit resistance to diet-induced obesity particularly in males. Third, the resistance to HFD-induced weight gain was not due to changes in food intake, energy absorption or physical activity, but appears to be due to increased energy expenditure as indicated by the elevated RMR, increased UCP1 mRNA and protein in BAT, and increased BAT sympathetic nerve activity. Fourth, there were only modest changes in glucose tolerance and insulin sensitivity in Ren-b^{Null} mice. However, sRA mice, which exhibit much higher brain RAS activity due to marked over-expression of human Ren-a (but not Ren-b) and human AGT in the brain, and exhibit larger increases in blood pressure, drinking and metabolic phenotypes than Ren-b^{Null} mice were particularly insulin sensitive.^{5,18}

Increased activity of the brain RAS has been implicated in many models of hypertension and this is most often associated with increased activity of the sympathetic nervous system.¹⁰ Increased sympathetic outflow in humans has been attributed to be the basis of the failure of antihypertensive therapy in some forms of resistant hypertension such as refractory hypertension.²⁰ Whether refractory hypertension or neurogenic hypertension in humans is due to increased activity of the brain RAS remains an unanswered question. Interestingly, we previously showed that the same brain-specific isoform of renin mRNA (Ren-b) expressed in the brain of mice and rats is also selectively expressed in the human brain suggesting its function may be conserved.¹³

We originally developed the hypothesis that Ren-b encodes an intracellular renin which may play a role in the generation of intracellular Ang-II. Conceptually, this hypothesis, if supported experimentally, could have provided the missing link defining Ang-II as a neurotransmitter.²¹ Indeed, Ang-II satisfies many of the requirements as a neurotransmitter, except the mechanism for its intracellular synthesis and sorting to the neurosecretory system was lacking.²² But instead of hypotension and resistance to high blood pressure, Ren-b^{Null} mice displayed hypertension.¹¹ Moreover, the increased arterial pressure was accompanied by increased activity of the brain RAS, as evidenced by increased expression of Ren-a and AT1 receptor mRNAs in some regions of the brain, and a robust depressor response to intracerebroventricular administration of either a renin-inhibitor, ACE inhibitor, or AT1 receptor blocker. Our data certainly does not experimentally rule out Ang-II as a neurotransmitter but did not provide additional support for intracellular synthesis through intracellular renin. Thus, this necessitated a reevaluation of the original concept. The findings that 1) expression of Ren-a, which is dormant in brain of normal mice, was increased in Ren-b^{Null} mice, and 2) Ren-a expression is increased and Ren-b expression is decreased in DOCA-salt hypertension suggested the possibility that this may occur naturally and play a regulatory role.¹⁴ Based on a preponderance of the evidence, we hypothesize that 1) there is a tight selective transcriptional regulation of Ren-b and Ren-a, and 2) disinhibition of Ren-a may occur in response to physiological or pathophysiological cues. However, the molecular mechanism whereby Ren-a disinhibition occurs remains unclear. We have reviewed possible mechanisms by which this transcriptional regulatory circuit could be operating.¹⁰

In the current study, Ren-b^{Null} mice exhibited normal intake of fluids under baseline and DOCA-salt conditions. It was not until the mice were provided a more potent stimulus, dehydration, before an increase in water intake was observed, and then primarily after DOCA-salt. Numerous studies, most recently optogenetics have implicated the subfornical organ (SFO) as an important regulator of fluid intake.^{23,24} Water deprivation increases neural activity in the SFO, along with other structures in the lamina terminalis.²⁵ We previously showed that increased synthesis of Ang-II specifically in the SFO is sufficient to induce water intake.^{26,27} There was no increase in total renin mRNA in the SFO of Ren-b^{Null} mice.¹¹ However, that there was maintenance of total renin mRNA expression in the SFO of Ren-b^{Null} mice implies there must have been a redistribution of renin mRNA isoforms from Ren-b to Ren-a. One possible interpretation of this is that Ren-b deficiency would provide an opportunity to increase the secretion of prorenin in the SFO which, perhaps in the presence of prorenin receptor, may cause local Ang-II synthesis.²⁸

Inconsistent with this interpretation was that Ren-b^{Null} mice did not exhibit increased water intake at baseline suggesting either that the level of Ang-II produced in Ren-b^{Null} mice is insufficient to increase drinking, or the increase occurred in regions of the brain unrelated to fluid homeostasis. Further studies employing conditional alleles of Ren-b (Ren-b^{Flox}) and Ren-a (Ren-a^{Flox}) will provide opportunities to examine the consequences of site-specific Ren-b deletion with Ren-a activation on drinking and other phenotypes.

Compared with fluid intake, much more dramatic effects were observed on body weight, particularly when mice were fed HFD. Although there were no differences in body weight in male or female Ren-b^{Null} mice fed a chow diet, male mice in particular exhibited a blunted increase in weight gain in response to HFD. Ren-b^{Null} mice also exhibited an increase in resting metabolic rate. We evaluated both male and female mice fed either chow or HFD and used ANCOVA to examine the relationship between RMR, measured by respirometry, over a wide range of body weights. Factors which influence measurements of RMR have been recently reviewed.²⁹ Consistent with the increase in RMR, BAT UCP1 mRNA and protein as well as SNA were significantly elevated in Ren-b^{Null} mice. Together, these observations imply an increase in thermogenesis in Ren-b^{Null} mice most likely initiated by increased sympathoexcitation to the BAT. Our data also imply increased Ang-II in a neural circuit controlling energy balance, and consistent with this, AT1 receptor expression was increased in the paraventricular nucleus (PVN) of Ren-b^{Null}.¹¹ The PVN is a major integrating center for both cardiovascular and metabolic responses and AT1 receptors have been localized in the PVN.^{30,31} As above, there was no increase in total renin mRNA in the arcuate nucleus, but again, the redistribution of Ren-a/Ren-b may provide a source of extracellular prorenin/renin needed for local Ang-II synthesis in this nucleus. This may be significant as AT1 receptor mRNA are localized on some leptin receptor-containing neurons in the arcuate nucleus which regulate RMR.⁸ Deletion of AT1 receptor in mice or inhibition of angiotensin production and action in the brain of rats blunts sympathetic activity to the kidney and BAT in response to centrally administered leptin.⁷ Thus, it would be interesting to assess if renin-mediated production of Ang-II in the arcuate nucleus is required to mediate SNA to thermogenic BAT.

One of the curious observations was that UCP1 and increased BAT SNA was observed in chow fed mice, but body weight was similar in chow fed control and Ren-b^{Null} mice. This could indicate that the increase in UCP1 expression is insufficient to affect adiposity and body weight at least when mice are fed a chow diet. However, we found that challenging mice with HFD revealed a difference in adiposity and body weight. Whether the decrease in weight gain and adiposity is mechanistically related to the increase in RMR remains unclear.

Perspectives

Disruption of Ren-b caused a modest but statistically significant reduction in glucose tolerance, and simultaneously caused a trend toward increased insulin sensitivity. In parallel, transgenic activation of the brain RAS in sRA mice resulted in a more robust increase in insulin sensitivity, as quantified by PET/CT imaging, presumably due to increased BAT SNA. These results complement our previous observation of increased glucose uptake in thermogenic adipose of sRA mice, assessed using radiolabeled glucose uptake

quantification.⁶ Along these lines it is interesting to note that RAS blockade has been reported to prevent insulin resistance.^{32–34} Similarly, in clinical trials, RAS blockade is more effective than other antihypertensives which do not target the RAS at improving insulin sensitivity.^{35,36} Other large clinical trials suggest benefit from RAS blockade on incidence of diabetes or glucose tolerance, or both.^{19,33,37} At first, our results in Ren-b^{Null} and sRA with increased brain RAS activity seem in contradiction to the clinical benefits of RAS inhibition. However, Ren-b^{Null} and sRA are both characterized by a decrease in systemic RAS activity (due to feedback inhibition caused by hypertension).^{5,11} We previously demonstrated that the coupling of reduced systemic (or circulating) RAS activity with increased sympathetic nerve activity to adipose tissue stimulates thermogenesis and resting metabolic rate.⁶ Further studies are clearly needed to assess if these observations can be translated therapeutically.

Supplementary Material

Refer to Web version on PubMed Central for supplementary material.

Acknowledgments

Transgenic mice were generated at the University of Iowa Gene Editing Facility supported by grants from the NIH and from the Carver College of Medicine. We thank Bill Paradee, Norma Sinclair, JoAnne Schwarting, and Patricia Yarolem for genotyping mice.

Sources of Funding: This work was supported through research grants from the National Institutes of Health (NIH) to CDS (HL084207), KR (HL084207), JLG (HL098276, HL134850), and grants from the American Heart Association to CDS (15SFRN23480000), KR (14EIA18860041), and NL (14PRE18330015), and the University of Iowa Fraternal Order of Eagles Diabetes Research Center to KR and JLG. In addition, the University of Iowa Small Animal Imaging Core is supported in part from an instrumentation grant (NIH 1S10RR025036-01) for equipment purchase with operational support from the cancer center support grant (NIH P30 CA086862). The authors gratefully acknowledge the generous research support of the Roy J. Carver Trust.

References

1. Simpson JB, Routtenberg A. Subfornical organ: site of drinking elicitation by angiotensin II. *Science*. 1973; 181:1772–1775.
2. Simpson JB, Routtenberg A. Subfornical organ: a dipsogenic site of action of angiotensin II. *Science*. 1978; 201:379–381. [PubMed: 663664]
3. Davisson RL, Oliverio MI, Coffman TM, Sigmund CD. Divergent Functions of Angiotensin II Receptor Isoforms in Brain. *J Clin Invest*. 2000; 106:103–106. [PubMed: 10880053]
4. Guyenet PG. The sympathetic control of blood pressure. *Nat Rev Neurosci*. 2006; 7:335–346. [PubMed: 16760914]
5. Grobe JL, Grobe CL, Beltz TG, et al. The Brain Renin-Angiotensin System Controls Divergent Efferent Mechanisms to Regulate Fluid and Energy Balance. *Cell Metabolism*. 2010; 12:431–442. [PubMed: 21035755]
6. Littlejohn NK, Keen HL, Weidemann BJ, et al. Suppression of Resting Metabolism by the Angiotensin AT2 Receptor. *Cell Rep*. 2016; 16:1548–1560. [PubMed: 27477281]
7. Hilzendege AM, Morgan DA, Brooks L, Dellsperger DJ, Liu X, Grobe JL, Rahmouni K, Sigmund CD, Mark AL. A Brain Leptin-Renin Angiotensin System Interaction in the Regulation of Sympathetic Nerve Activity. *Am J Physiol: Heart and Circulatory Physiology*. 2012; 303:H197–H206.
8. Claflin KE, Sandgren JA, Lambert AM, Weidemann BJ, Littlejohn NK, Burnett CM, Pearson NA, Morgan DA, Gibson-Corley KN, Rahmouni K, Grobe JL. Angiotensin AT1A receptors on leptin receptor-expressing cells control resting metabolism. *J Clin Invest*. 2017; 127:1414–1424. [PubMed: 28263184]

9. Marc Y, Llorens-Cortes C. The role of the brain renin-angiotensin system in hypertension: implications for new treatment. *Prog Neurobiol.* 2011; 95:89–103. [PubMed: 21763394]
10. Nakagawa P, Sigmund CD. How Is the Brain Renin-Angiotensin System Regulated? *Hypertension.* 2017; 70:10–18. [PubMed: 28559391]
11. Shinohara K, Liu X, Morgan DA, Davis DR, Sequeira-Lopez ML, Cassell MD, Grobe JL, Rahmouni K, Sigmund CD. Selective Deletion of the Brain-Specific Isoform of Renin Causes Neurogenic Hypertension. *Hypertension.* 2016; 68:1385–1392. [PubMed: 27754863]
12. Lee-Kirsch MA, Gaudet F, Cardoso MC, Lindpaintner K. Distinct renin isoforms generated by tissue-specific transcription initiation and alternative splicing. *Circ Res.* 1999; 84:240–246. [PubMed: 9933256]
13. Sinn PL, Sigmund CD. Identification of Three Human Renin mRNA Isoforms Resulting from Alternative Tissue-Specific Transcriptional Initiation. *Physiol Genomics.* 2000; 3:25–31. [PubMed: 11015597]
14. Grobe JL, Rahmouni K, Liu X, Sigmund CD. Metabolic rate regulation by the renin-angiotensin system: brain vs. body. *Pflugers Arch.* 2013; 465:167–175. [PubMed: 22491893]
15. Itaya Y, Suzuki H, Matsukawa S, Kondo K, Saruta T. Central renin-angiotensin system and the pathogenesis of DOCA-salt hypertension in rats. *Am J Physiol.* 1986; 251:H261–H268. [PubMed: 3526927]
16. Kubo T, Yamaguchi H, Tsujimura M, Hagiwara Y, Fukumori R. Blockade of angiotensin receptors in the anterior hypothalamic preoptic area lowers blood pressure in DOCA-salt hypertensive rats. *Hypertens Res.* 2000; 23:109–118. [PubMed: 10770257]
17. Grobe JL, Buehrer BA, Hilzendeger AM, Liu X, Davis DR, Xu D, Sigmund CD. Angiotensinergic signaling in the brain mediates metabolic effects of deoxycorticosterone (DOCA)-salt in C57 mice. *Hypertension.* 2011; 57:600–607. [PubMed: 21263123]
18. Sakai K, Agassandian K, Morimoto S, Sinnayah P, Cassell MD, Davisson RL, Sigmund CD. Local production of angiotensin II in the subfornical organ causes elevated drinking. *J Clin Invest.* 2007; 117:1088–1095. [PubMed: 17404622]
19. Underwood PC, Adler GK. The renin angiotensin aldosterone system and insulin resistance in humans. *Curr Hypertens Rep.* 2013; 15:59–70. [PubMed: 23242734]
20. Acelajado MC, Pisoni R, Dudenbostel T, Dell'Italia LJ, Cartmill F, Zhang B, Cofield SS, Oparil S, Calhoun DA. Refractory hypertension: definition, prevalence, and patient characteristics. *J Clin Hypertens (Greenwich).* 2012; 14:7–12. [PubMed: 22235818]
21. Grobe JL, Xu D, Sigmund CD. An intracellular renin-angiotensin system in neurons: fact, hypothesis, or fantasy. *Physiology.* 2008; 23:187–193. [PubMed: 18697992]
22. Ferguson AV, Washburn DL, Latchford KJ. Hormonal and neurotransmitter roles for angiotensin in the regulation of central autonomic function. *Exp Biol Med (Maywood).* 2001; 226:85–96. [PubMed: 11446443]
23. Matsuda T, Hiyama TY, Niimura F, Matsusaka T, Fukamizu A, Kobayashi K, Kobayashi K, Noda M. Distinct neural mechanisms for the control of thirst and salt appetite in the subfornical organ. *Nat Neurosci.* 2017; 20:230–241. [PubMed: 27991901]
24. Zimmerman CA, Lin YC, Leib DE, Guo L, Huey EL, Daly GE, Chen Y, Knight ZA. Thirst neurons anticipate the homeostatic consequences of eating and drinking. *Nature.* 2016; 537:680–684. [PubMed: 27487211]
25. De Luca LAJ, Xu Z, Schoorlemmer GH, Thunhorst RL, Beltz TG, Menani JV, Johnson AK. Water deprivation-induced sodium appetite: humoral and cardiovascular mediators and immediate early genes. *Am J Physiol Regul Integr Comp Physiol.* 2002; 282:R552–R559. [PubMed: 11792666]
26. Coble JP, Cassell MD, Davis DR, Grobe JL, Sigmund CD. Activation of the Renin-Angiotensin System Specifically in the Subfornical Organ is Sufficient to Induce Fluid Intake. *Am J Physiol Regul Integr Comp Physiol.* 2014; 307:R376–R386. [PubMed: 24965793]
27. Coble JP, Johnson RF, Cassell MD, Johnson AK, Grobe JL, Sigmund CD. Activity of PKC-alpha within the Subfornical Organ is Necessary for Fluid Intake due to Brain Angiotensin. *Hypertension.* 2014; 64:141–148. [PubMed: 24777977]

28. Li W, Sullivan MN, Zhang S, Worker CJ, Xiong Z, Speth RC, Feng Y. Intracerebroventricular infusion of the (Pro)renin receptor antagonist PRO20 attenuates deoxycorticosterone acetate-salt-induced hypertension. *Hypertension*. 2015; 65:352–361. [PubMed: 25421983]
29. Grobe JL. Comprehensive Assessments of Energy Balance in Mice. *Methods Mol Biol*. 2017; 1614:123–146. [PubMed: 28500600]
30. Contreras C, Nogueiras R, Dieguez C, Rahmouni K, Lopez M. Traveling from the hypothalamus to the adipose tissue: The thermogenic pathway. *Redox Biol*. 2017; 12:854–863. [PubMed: 28448947]
31. de Kloet AD, Wang L, Pitra S, Hiller H, Smith JA, Tan Y, Nguyen D, Cahill KM, Sumners C, Stern JE, Krause EG. A Unique “Angiotensin-Sensitive” Neuronal Population Coordinates Neuroendocrine, Cardiovascular, and Behavioral Responses to Stress. *J Neurosci*. 2017; 37:3478–3490. [PubMed: 28219987]
32. Abuissa H, Jones PG, Marso SP, O’Keefe JH Jr. Angiotensin-converting enzyme inhibitors or angiotensin receptor blockers for prevention of type 2 diabetes: a meta-analysis of randomized clinical trials. *J Am Coll Cardiol*. 2005; 46:821–826. [PubMed: 16139131]
33. Group NS, McMurray JJ, Holman RR, et al. Effect of valsartan on the incidence of diabetes and cardiovascular events. *N Engl J Med*. 2010; 362:1477–1490. [PubMed: 20228403]
34. van der Zijl NJ, Moors CC, Goossens GH, Hermans MM, Blaak EE, Diamant M. Valsartan improves {beta}-cell function and insulin sensitivity in subjects with impaired glucose metabolism: a randomized controlled trial. *Diabetes Care*. 2011; 34:845–851. [PubMed: 21330640]
35. Jin HM, Pan Y. Angiotensin type-1 receptor blockade with losartan increases insulin sensitivity and improves glucose homeostasis in subjects with type 2 diabetes and nephropathy. *Nephrol Dial Transplant*. 2007; 22:1943–1949. [PubMed: 17308317]
36. Grassi G, Seravalle G, Dell’Oro R, Trevano FQ, Bombelli M, Scopelliti F, Facchini A, Mancia G, Study C. Comparative effects of candesartan and hydrochlorothiazide on blood pressure, insulin sensitivity, and sympathetic drive in obese hypertensive individuals: results of the CROSS study. *J Hypertens*. 2003; 21:1761–1769. [PubMed: 12923410]
37. Investigators DT, Bosch J, Yusuf S, Gerstein HC, Pogue J, Sheridan P, Dagenais G, Diaz R, Avezum A, Lanus F, Probstfield J, Fodor G, Holman RR. Effect of ramipril on the incidence of diabetes. *N Engl J Med*. 2006; 355:1551–1562. [PubMed: 16980380]

Novelty and Significance

What Is New?

- The brain specific isoform of renin (Ren-b) regulates the activity of the brain renin-angiotensin system by tightly controlling expression of Ren-a encoding preprorenin.
- Selective deletion of Ren-b in the brain disinhibits expression of the renin-a.
- We examined if deletion of Ren-b alterations fluid intake and metabolism.

What Is Relevant?

- Dehydration promoted increased water intake in Ren-b^{Null} mice.
- When fed a high fat diet, male Ren-b^{Null} mice gained significantly less weight than control mice, an effect blunted in female mice.
- Male Ren-b^{Null} mice exhibited increased thermogenesis due to an increase in sympathetic nerve activity to the interscapular brown adipose tissue.

Summary

- These data support the hypothesis that the brain RAS regulates energy homeostasis by stimulating sympathoexcitation of thermogenic brown adipose tissue and increasing resting metabolic rate.

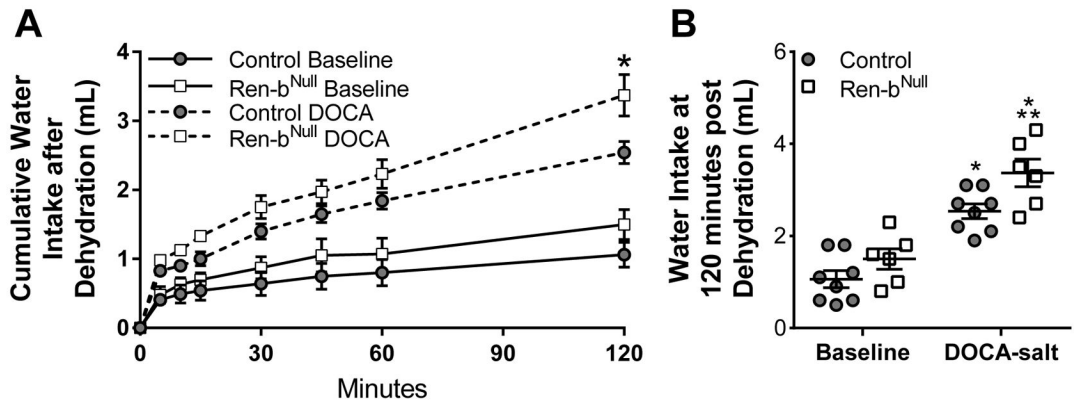


Figure 1. Water Intake

A) Water intake was measured before and after DOCA-salt treated control and Ren-b^{Null} mice both subjected to 18 hours of water deprivation. The same cohort of mice was analyzed in the baseline period and 21 days later after DOCA-salt (control n=8; Ren-b^{Null} n=6). Water intake was measured at the indicated times and cumulative water intake is plotted vs time in mice singly housed in metabolic cages. B) Cumulative water intake at 120 minutes from the experiment presents in A is shown. All data represent mean \pm SEM analyzed by 2-way ANOVA. ANOVA Results: Genotype: P=0.007; DOCA: P<0.001; Genotype X DOCA: P=0.37; Tukey's Multiple Comparisons Test: *, P<0.05 DOCA-salt vs baseline; **, P<0.05 vs Ren-b vs. control.

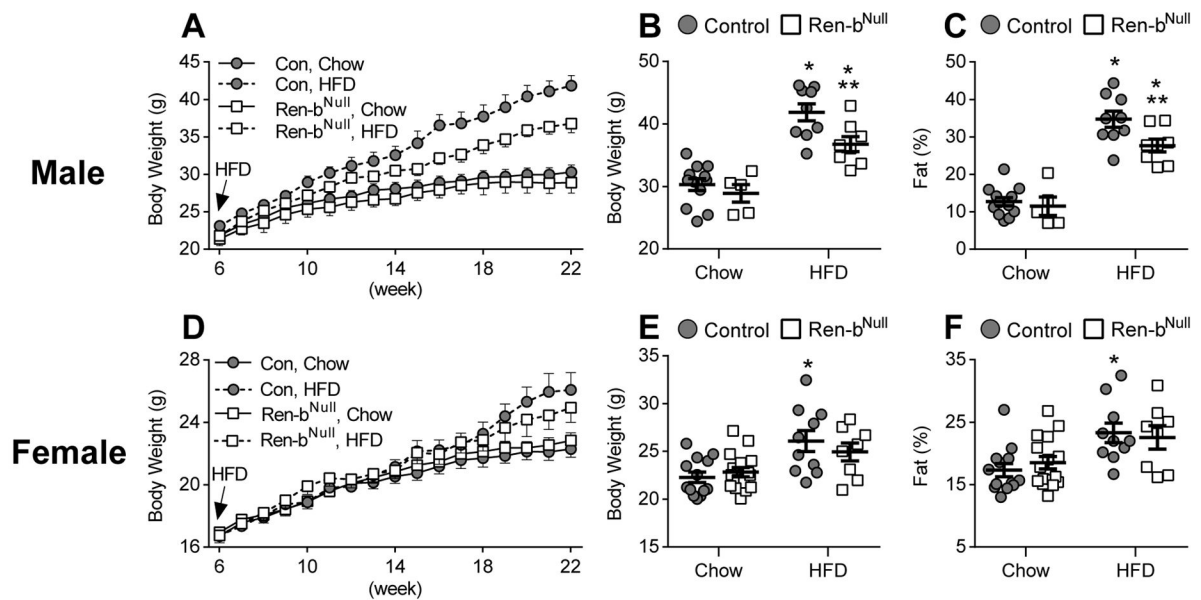


Figure 2. Body Weight

A) Body weight of male mice fed normal chow or high-fat diet (HFD) from 6–22 weeks of age (control chow n=12; Ren-b^{Null} chow n=5; control HFD n=9; Ren-b^{Null} HFD n=8). B–C) Body weight (B) and % fat mass (C) of male mice fed normal chow or HFD at 22 weeks of age. ANOVA Results BW: Genotype: P=0.016; Diet: P<0.001; Genotype X Diet: P=0.15; ANOVA Results %Fat: Genotype: P=0.032; Diet: P<0.001; Genotype X Diet: P=0.12; Tukey’s Multiple Comparisons Test: *, P<0.05 HFD vs baseline; **, P<0.05 vs Ren-b vs. control. D) Body weight of female mice fed normal chow or high-fat diet (HFD) 6–22 weeks of age. HFD was started at 6 weeks of age (control chow n=13; Ren-b^{Null} chow n=16; control HFD n=10, Ren-b^{Null} HFD n=8). E–F) Body weight (E) and % fat mass (F) of female mice fed normal chow or HFD at 22 weeks of age. ANOVA Results BW: Genotype: P=0.79; Diet: P=0.003; Genotype X Diet: P=0.27; ANOVA Results %Fat: Genotype: P=0.86; Diet: P=0.004; Genotype X Diet: P=0.47; Tukey’s Multiple Comparisons Test: *, P<0.05 HFD vs baseline; **, P<0.05 vs Ren-b vs. control.

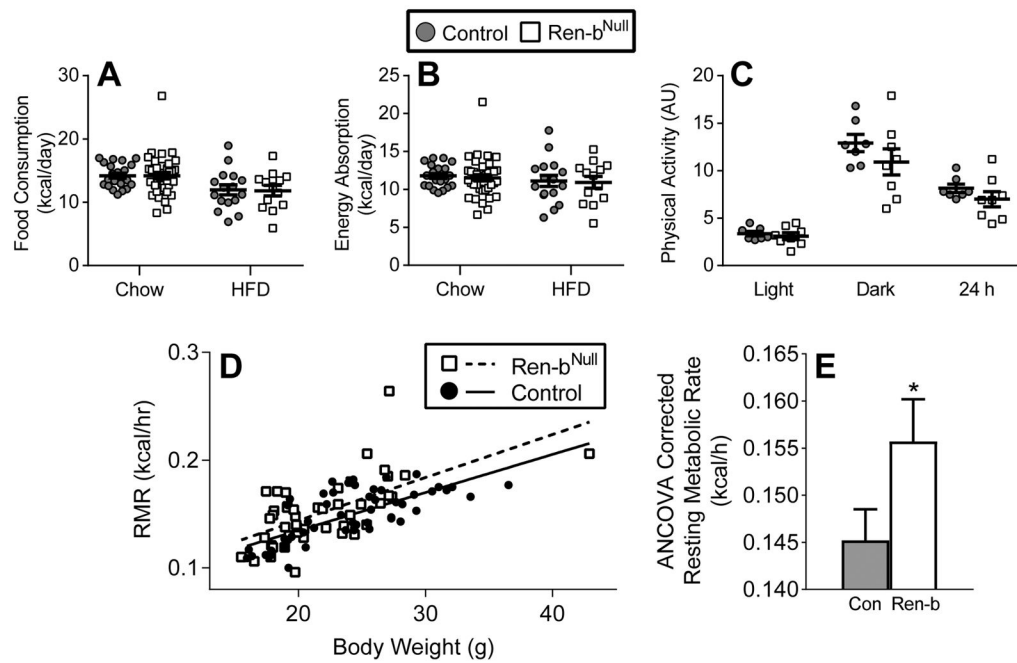


Figure 3. Metabolic Analyses

Energy consumption (A) and absorption (B) was measured in male mice (control chow n=22; Ren-b^{Null} chow n=37; control HFD n=16; Ren-b^{Null} HFD n=13). All data represent mean \pm SEM. ANOVA Results Food Consumption: Genotype: P=0.92; Diet: P=0.001; Genotype X Diet: P=0.92; ANOVA Results Energy Absorption: Genotype: P=0.70; Diet: P=0.27; Genotype X Diet: P=0.96. C) Physical activity as measured by radiotelemetry was measured in male mice fed a chow diet (control n=7; Ren-b^{Null} n=8). Data was evaluated by t-test during light (P=0.55), dark (P=0.26) and 24 hour (P=0.25) comparing control to Ren-b^{Null}. D) Resting metabolic rate was measured by respirometry in control (n=53 consisting of 22 males fed chow, 7 males fed HFD, 19 females fed chow, 5 females fed HFD) and Ren-b^{Null} (n=46 consisting of 11 males fed chow, 4 males fed HFD, 22 females fed chow, 9 females fed HFD) mice. E) ANCOVA analysis of the data presented in D. *, P=0.015 by genotype; P=0.57 by sex; P=0.99 by diet; P=0.46 genotype \times sex interaction; P=0.42 genotype \times diet interaction.

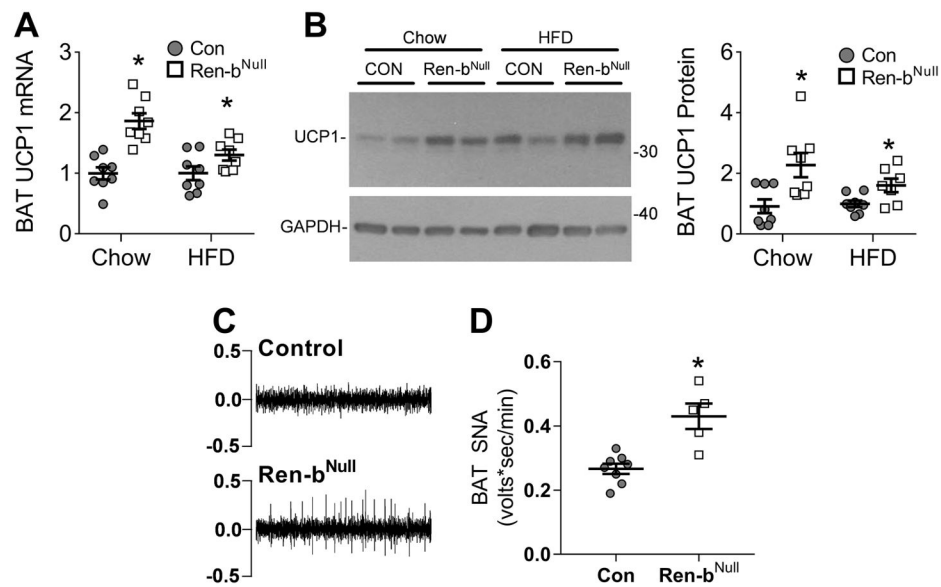


Figure 4. UCP1 Expression and Inguinal BAT SNA

A) UCP1 mRNA expression in interscapular BAT of male mice fed normal chow or HFD (n=8 per group). Data were independently analyzed comparing UCP1 mRNA in chow fed Ren-b^{Null} vs control and HFD fed renin-b^{Null} vs control. *, P<0.05 vs control analyzed by t-test. B) Representative western blot of UCP1 protein expression in interscapular BAT of mice fed normal chow or HFD. Quantification of Western blot experiments consisting of control fed chow (n=8), renin-b^{Null} fed chow (n=8), control fed HFD (n=8), and Ren-b^{Null} fed HFD (n=7). *, P<0.05 vs control analyzed by t-test. C) Representative raw tracings of BAT SNA in control and Ren-b^{Null} mice. D) Basal BAT SNA (control n=8, Ren-b^{Null} mice n=5). *P<0.05 vs control by t-test. All data represent mean \pm SEM.

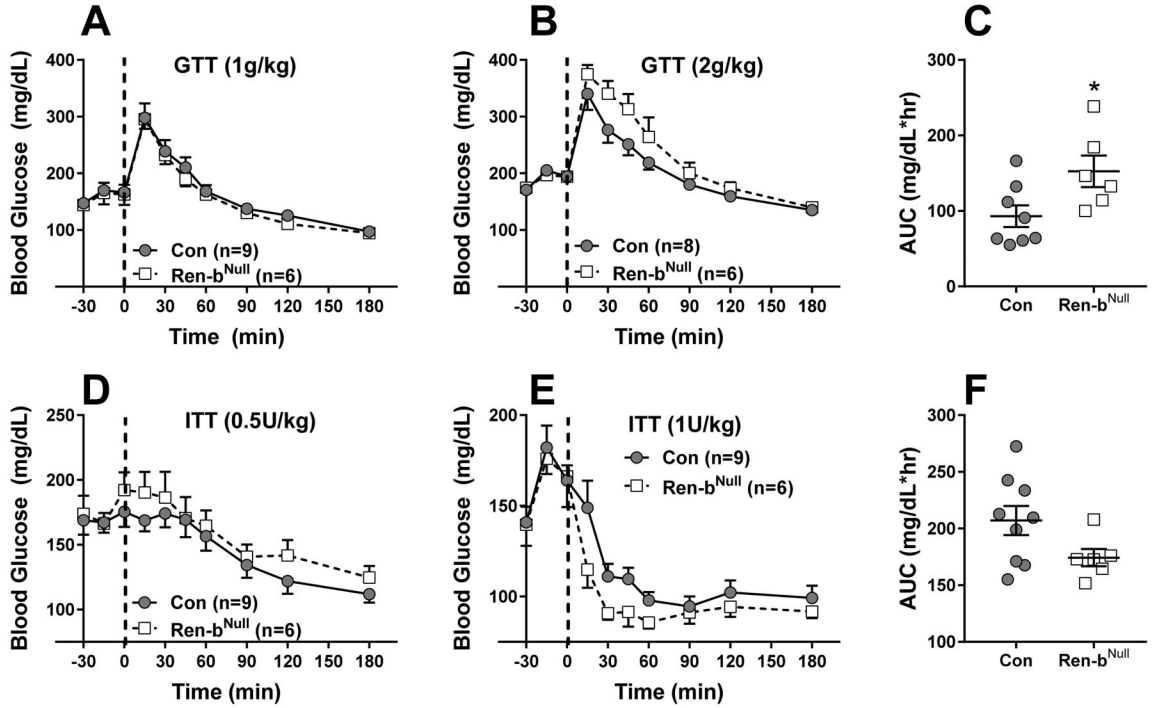


Figure 5. Glucose Homeostasis in Ren-b-deficient Mice

A) Glucose tolerance tests (GTT; A,B) and insulin tolerance tests (ITT; D,E) were performed in male control and Ren-b^{Null} mice (A–F) using the indicated dose of glucose or insulin. The sample sizes are indicated. ANOVA Results GTT (2g/kg): Genotype: P=0.16; Time: P<0.001; Genotype X Time: P=0.037. ANOVA Results ITT (1U/kg): Genotype: P=0.23; Time: P<0.001; Genotype X Time: P=0.27. C and F reflect the area under the curve (AUC) for data in panels B and E, respectively. *, P=0.03 Ren-b vs control by t-test. Data plotted are mean ± SEM.

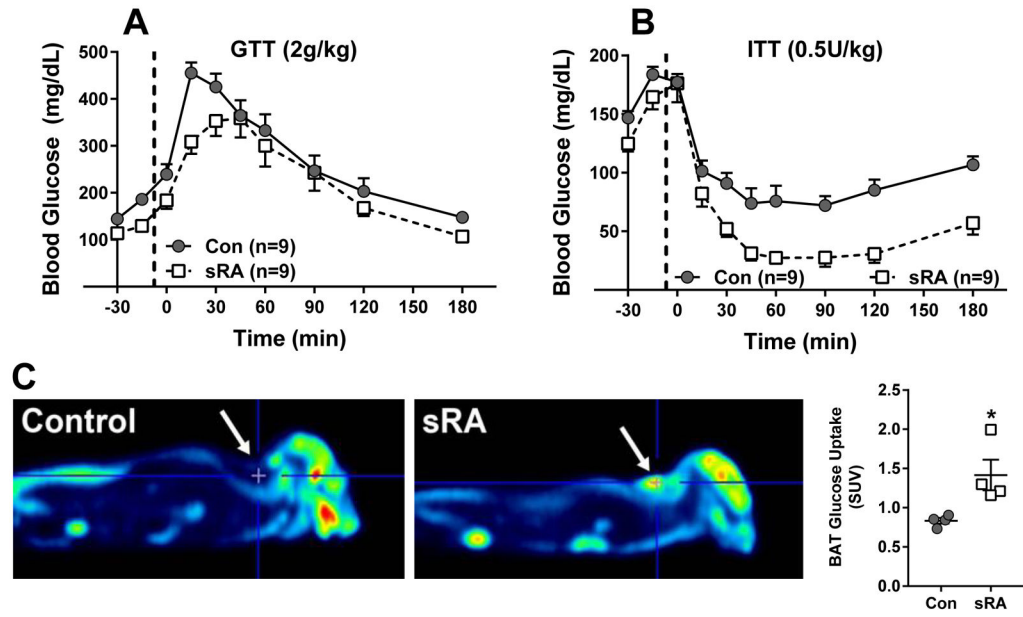


Figure 6. Glucose Homeostasis in sRA Mice

A) Glucose tolerance test (GTT; A) and insulin tolerance test (ITT; B) were performed in male sRA and littermate controls (fed chow, 8–12 weeks of age) using the indicated dose of glucose or insulin. The sample sizes are indicated. ANOVA Results GTT: Genotype: $P=0.09$; Time: $P<0.001$; Genotype X Time: $P=0.025$. AUC: $P=0.52$; ANOVA Results ITT: Genotype: $P<0.001$; Time: $P<0.001$; Genotype X Time: $P=0.013$; AUC: $P=0.017$ Data plotted are mean \pm SEM. C) Glucose uptake was measured by PET ($n=4$ per group, 8–12 weeks of age) and quantified as described in the Methods. SUV refers to standardized uptake value units of [^{18}F]Fluorodeoxyglucose. Data plotted are mean \pm SEM. * $P<0.03$ sRA vs control by t-test.